

A Comparative Study of the Harmonic and Arithmetic Averaging of Diffusion Coefficients for Non-Linear Heat Conduction Problems

Samet Y. Kadioglu
Robert R. Nourgaliev
Vincent A. Mousseau

March 2008



The INL is a U.S. Department of Energy National Laboratory
operated by Battelle Energy Alliance

A Comparative Study of the Harmonic and Arithmetic Averaging of Diffusion Coefficients for Non-Linear Heat Conduction Problems

**Samet Y. Kadioglu
Robert R. Nourgaliev
Vincent A. Mousseau**

March 2008

**Idaho National Laboratory
Idaho Falls, Idaho 83415**

**Prepared for the
U.S. Department of Energy
Through the INL LDRD Program
Under DOE Idaho Operations Office
Contract DE-AC07-05ID14517**

A Comparative Study of The Harmonic and Arithmetic Averaging of Diffusion Coefficients for Non-linear Heat Conduction Problems

March 11, 2008

Samet Y. Kadioglu, Robert R. Nourgaliev, Vincent A. Mousseau,

Reactor Physics Analysis & Design, Idaho National Laboratory, P. O.
Box 1625, MS 3840, Idaho Falls, ID 83415

Contents

1	Abstract	3
2	Introduction	4
3	Model equation	5
4	Numerical Algorithm	5
4.1	The Harmonic Average Model	5
4.2	The Arithmetic Average Model	7
4.3	Truncation error analysis	9
5	Numerical results	11
5.1	Moving-front Single-material test	11
5.2	Stationary-interface Multi-material test	13
6	Conclusion	14

1 Abstract

We perform a comparative study for the harmonic versus arithmetic averaging of the heat conduction coefficient when solving non-linear heat transfer problems. In literature, the harmonic average is the method of choice, because it is widely believed that the harmonic average is more accurate model. However, our analysis reveals that this is not necessarily true. For instance, we show a case in which the harmonic average is less accurate when a coarser mesh is used. More importantly, we demonstrated that if the boundary layers are finely resolved, then the harmonic and arithmetic averaging techniques are identical in the truncation error sense. Our analysis further reveals that the accuracy of these two techniques depends on how the physical problem is modeled.

2 Introduction

In this paper, we study how the choice of averaging of the heat conduction coefficient affects the solutions of non-linear heat conduction problems. In literature, the harmonic average is widely used by the heat transfer community. The harmonic average was promoted by Patankar [7]. It is designed to solve heat transfer problems involving multiple material properties. Patankar [7] concluded that the harmonic average is more accurate in his case studies. Since then, the harmonic average became people's choice when dealing with non-linear heat conduction problems. To our knowledge, the harmonic average is always assumed to be more accurate model regardless of the problem types, therefore no comparative study has been performed on this matter.

In this paper, we compare the harmonic average model with the arithmetic average model. We provide in-depth mathematical analysis and numerical computations. Our analysis and numerical results reveal that both models are identical for a very fine mesh. However, for coarser grids, in some cases the harmonic average is better, in others the arithmetic average is better. For instance, in a single material test case, the harmonic average for coarser grids performs very poorly to predict the thermal wave front location. On the other hand, the harmonic average (again for coarser grids) is found to be more accurate when dealing with multi-material test cases. In Section 4, we provide a detail mathematical analysis about the accuracy of the two models. Our analysis shows that the averaging techniques and the model problems are tightly related. In other words, the model problem and the choice of averaging will directly affect the accuracy. Therefore, one should always be aware of the suitability of the averaging technique to the model problem he/she is dealing with. A different way of stating this is that the averaging technique is a sub-grid physics model. The sub-grid physics models are based on different assumptions. If these assumptions are matched in solving the problem, then the model will be more accurate.

The organization of the present paper is as follows. In Section 3, we describe the partial differential equations of our model. In Section 4, we describe the numerical algorithm employed and provide several mathematical derivations and analysis. In Section 5, we present numerical results involving single and multi-material test cases. Finally, Section 6 contains concluding remarks.

3 Model equation

We consider the following model equation,

$$\frac{\partial T}{\partial t} + \frac{\partial}{\partial x} \left(D \frac{\partial T}{\partial x} \right) = 0, \quad (1)$$

representing a non-linear heat conduction problem. Where D is the non-linear heat conduction coefficient. In our particular case, we define D as $D = T^a$. Here the constant a determines the strength of the non-linearity. (Note that setting $a = 0$ turns (1) into the linear diffusion equation). The variation in the heat conduction coefficient creates a fast moving wave front. This phenomena is also known as the *Marshak wave* ([5],[3]).

4 Numerical Algorithm

Our numerical algorithm is second order in both space and time, i.e, it is based on the Crank-Nicolson scheme [9]. Our space discretization is done conservatively based on a second order finite volume technique ([4],[10]). Our time integration is based on the Jacobien-Free Newton Krylov method [2].

The time and space discretization of Eqn. (1) can be written as:

$$\frac{T_i^{n+1} - T_i^n}{\Delta t} + \frac{D_{i+1/2}^{n+1}(T_x)_{i+1/2}^{n+1} - D_{i-1/2}^{n+1}(T_x)_{i-1/2}^{n+1}}{\Delta x} = 0 \quad (2)$$

where

$$(T_x)_{i+1/2}^{n+1} = \frac{T_{i+1}^{n+1} - T_i^{n+1}}{\Delta x}. \quad (3)$$

The conductivity terms $D_{i+1/2}$ and $D_{i-1/2}$ are computed according to the harmonic or arithmetic averaging models.

4.1 The Harmonic Average Model

In this section, we show the derivation of the harmonic averaging of the heat conduction coefficient. Our derivation is based on two assumptions:

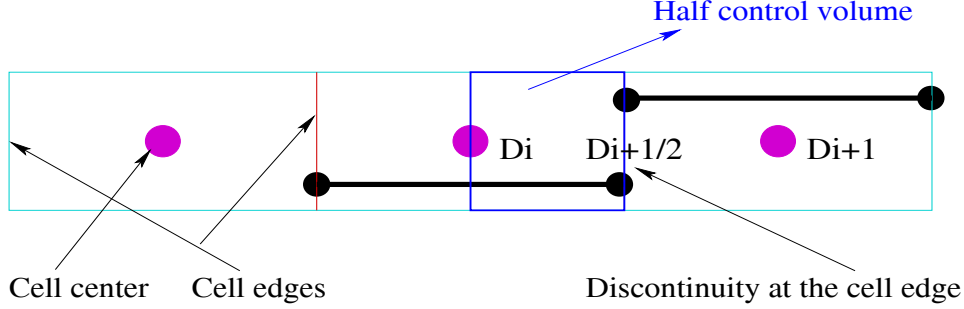


Figure 1: Conductivity representation for the harmonic average.

1) We assume the heat conduction coefficient is piecewise constant and continuous from cell edge to cell edge (refer to Figure 1). 2) We consider steady-state solutions.

We know that the flux-in is equal to the flux-out at the $(i + 1/2)$ face. From our first assumption, we also know that the conductivity terms (e.g., D 's) are equal from the cell center $(i + 1)$ to the cell edge $(i + 1/2)$, and from the cell edge $(i + 1/2)$ to the $(i)^{th}$ cell (refer to Figure 1). Then we can write

$$D_{i+1} \frac{T_{i+1} - T_{i+1/2}}{\Delta x/2} = D_i \frac{T_{i+1/2} - T_i}{\Delta x/2}. \quad (4)$$

Solving Eqn. (4) for $T_{i+1/2}$, we get

$$T_{i+1/2} = \frac{D_{i+1}T_{i+1} + D_iT_i}{D_{i+1} + D_i}. \quad (5)$$

Now, we consider the following conservative discretizations;

$$\frac{T_{i+1/4}^{n+1} - T_{i+1/4}^n}{\Delta t} - \frac{D_{i+1/2}T_{x,i+1/2} - D_iT_{x,i}}{\Delta x/2} = 0, \quad (6)$$

$$\frac{T_{i+1/2}^{n+1} - T_{i+1/2}^n}{\Delta t} - \frac{D_{i+1}T_{x,i+1} - D_iT_{x,i}}{\Delta x} = 0. \quad (7)$$

Here, Eqn. (6) corresponds to the conservation law when considering the left half part region between the $(i)^{th}$ and $(i+1)^{th}$ cells as the control volume (e.g., Figure 1). Eqn. (7) corresponds to the conservation law when considering

the whole region between the $(i)^{th}$ and $(i + 1)^{th}$ cells as the control volume. At the steady state, the time part of Eqn. (6) and Eqn. (7) vanishes. Then, we can write

$$D_i T_{x,i} = D_{i+1} T_{x,i+1} = D_{i+1/2} T_{x,i+1/2}. \quad (8)$$

Now, considering the discretization of Eqn (8) in half and whole control volumes using forward differencing, we have

$$D_{i+1} \frac{T_{i+1} - T_i}{\Delta x} = D_{i+1/2} \frac{T_{i+1/2} - T_i}{\Delta x/2}. \quad (9)$$

Using this result and assumption 1), we arrive at

$$D_{i+1/2} \frac{T_{i+1} - T_i}{\Delta x} = D_i \frac{T_{i+1/2} - T_i}{\Delta x/2}. \quad (10)$$

Substituting Eqn. (5) in Eqn.(10) and performing the necessary algebra we obtain

$$D_{i+1/2} = \frac{2D_i D_{i+1}}{D_i + D_{i+1}}. \quad (11)$$

Eqn. (11) is called the harmonic average of the conductivity term at the $(i + 1/2)^{th}$ face.

4.2 The Arithmetic Average Model

The arithmetic average is derived based on the assumption that the conductivity term is piecewise constant and continuous from cell center to cell center (refer to Figure 2). This assumption and knowing that the flux-in is equal to the flux-out at the $(i + 1/2)$ face give

$$D_{i+1/2} \frac{T_{i+1} - T_{i+1/2}}{\Delta x/2} = D_{i+1/2} \frac{T_{i+1/2} - T_i}{\Delta x/2}. \quad (12)$$

Solving Eqn. (12) for $T_{i+1/2}$, we get

$$T_{i+1/2} = \frac{T_{i+1} + T_i}{2}. \quad (13)$$

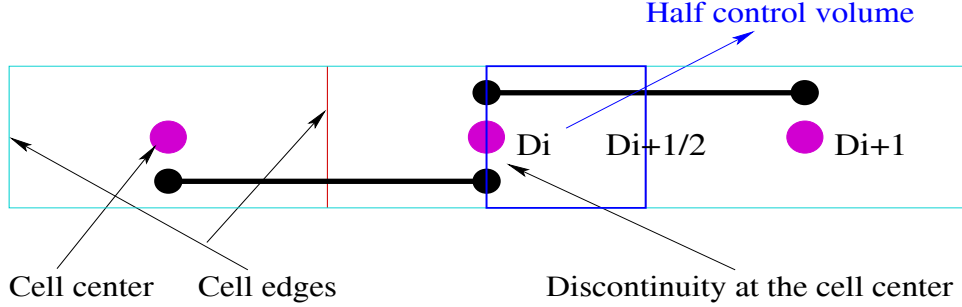


Figure 2: Conductivity representation for the arithmetic average.

Now, making use of the steady state assumption and considering fluxes in the left/right half and the whole control volumes (as we did in the harmonic case), we have

$$D_{i+1} \frac{T_{i+1} - T_i}{\Delta x} = D_{i+1/2} \frac{T_{i+1} - T_{i+1/2}}{\Delta x/2}, \quad (14)$$

$$D_i \frac{T_{i+1} - T_i}{\Delta x} = D_{i+1/2} \frac{T_{i+1/2} - T_i}{\Delta x/2}. \quad (15)$$

Adding Eqn. (14) and (15) from each side, we obtain

$$D_{i+1/2} = \frac{D_i + D_{i+1}}{2}. \quad (16)$$

Eqn. (16) is called the arithmetic average of the conductivity term at the $(i + 1/2)^{th}$ face.

Remark-1: We remark that the assumptions we made in Sections 4.1 and 4.2 are rather severe. For instance the constant conductivity term assumption would make sense for very fine grids. Furthermore, both models are derived at the steady state. Therefore, during the transient, we should expect more errors associated with the model itself. We observed these behaviors in our numerical results. For instance, in the single-material test case (Section 5.1), the harmonic model has more uncertainties for coarser grids leading more inaccuracies. On the other hand, in the multi-material test case, although the harmonic average is designed for this type of problem, during the transient, we don't see significant advantages. However, at the steady state the har-

monic average is many order of magnitude better since all of the assumptions we have made are matched (refer to Section 5.2).

Remark-2: Suppose, we have an insulator in the system, i.e, assume the $i + 1/2^{th}$ face corresponds to the boundary between the conductive material on the left and the insulator on the right. Then, $D_{i+1} \rightarrow 0$ in Eqn. (11), leading $D_{i+1/2} \rightarrow 0$. This means *zero* heat flux at the $i + 1/2^{th}$ face as it should. However, Eqn. (16) gives *none-zero* heat flux as $D_{i+1} \rightarrow 0$. Therefore, the harmonic average is the better choice (of course, one can simply set the flux to zero at the insulator as a boundary condition), if we are interested in complete insulation.

Remark-3: In a radiation diffusion problem, if $T_i > T_{i+1}$, then $D_i \gg D_{i+1}$, since typically $D(T) = T^3$. With these, the harmonic average will favor the lowest conduction coefficient, then this will artificially damp the radiation and not allow it to flow into cold zones [6]. So in this case, the harmonic average is not the way to go. The arithmetic average or weighted arithmetic and geometric averages are suggested in [6]. Using the combination of the averaging techniques is suggested in some other type of applications, e.g, shape optimization [1].

4.3 Truncation error analysis

In this section, we perform a truncation error analysis (refer to [9],[8]) for the two averaging techniques. The purpose of this analysis is to have a mathematical understanding about the errors committed by the two methods.

For the time being, we freeze the time discretization part of the PDE(i.e, our interest is the spatial error committed by the two models.). Then the PDE becomes

$$\frac{\partial}{\partial x} \left(D \frac{\partial T}{\partial x} \right) = 0. \quad (17)$$

Discrete form of this equation can be written as;

$$\frac{1}{\Delta x^2} [D_{i+1/2}(T_{i+1} - T_i) - D_{i-1/2}(T_i - T_{i-1})] = 0. \quad (18)$$

The harmonic average:

The harmonic average considers continuous fluxes across the cell centers (Figure 1), thus we perform Taylor series expansions centered at cell centers. We consider the following Taylor series expansions;

$$T_{i+1} = T_i + \Delta x T_{x,i} + \frac{\Delta x^2}{2} T_{xx,i} + \frac{\Delta x^3}{6} T_{xxx,i} + \frac{\Delta x^4}{24} T_{xxxx,i} \quad (19)$$

$$T_{i-1} = T_i - \Delta x T_{x,i} + \frac{\Delta x^2}{2} T_{xx,i} - \frac{\Delta x^3}{6} T_{xxx,i} + \frac{\Delta x^4}{24} T_{xxxx,i} \quad (20)$$

$$D_{i+1/2} = D_i + \frac{\Delta x}{2} D_{x,i} + \frac{\Delta x^2}{8} D_{xx,i} + \frac{\Delta x^3}{48} D_{xxx,i} + \frac{\Delta x^4}{384} D_{xxxx,i} \quad (21)$$

$$D_{i-1/2} = D_i - \frac{\Delta x}{2} D_{x,i} + \frac{\Delta x^2}{8} D_{xx,i} - \frac{\Delta x^3}{48} D_{xxx,i} + \frac{\Delta x^4}{384} D_{xxxx,i}. \quad (22)$$

Substituting these series expansions into Eqn. (18), canceling the common terms with opposite signs, and making use of Eqn. (17), we obtain

$$\tau_i = \frac{\Delta x^2}{24} [D_{x,i} T_{xxx,i} + D_i T_{xxxx,i}] + O(\Delta x^4). \quad (23)$$

This is the truncation error for the harmonic average.

The arithmetic average:

The arithmetic average considers continuous fluxes across the cell edges (Figure 2), thus we expand Taylor series centered at cell edges. We consider the following Taylor series expansions where we linearize at cell edges $i + 1/2$ and $i - 1/2$;

$$\begin{aligned} T_i = T_{i+1/2} & - \frac{\Delta x}{2} T_{x,i+1/2} + \frac{\Delta x^2}{8} T_{xx,i+1/2} - \frac{\Delta x^3}{48} T_{xxx,i+1/2} \\ & + \frac{\Delta x^4}{384} T_{xxxx,i+1/2} - \frac{\Delta x^5}{3840} T_{xxxxx,i+1/2} \end{aligned} \quad (24)$$

$$\begin{aligned} T_{i+1} = T_{i+1/2} & + \frac{\Delta x}{2} T_{x,i+1/2} + \frac{\Delta x^2}{8} T_{xx,i+1/2} + \frac{\Delta x^3}{48} T_{xxx,i+1/2} \\ & + \frac{\Delta x^4}{384} T_{xxxx,i+1/2} + \frac{\Delta x^5}{3840} T_{xxxxx,i+1/2} \end{aligned} \quad (25)$$

$$\begin{aligned}
T_i = T_{i-1/2} &+ \frac{\Delta x}{2} T_{x,i-1/2} + \frac{\Delta x^2}{8} T_{xx,i-1/2} + \frac{\Delta x^3}{48} T_{xxx,i-1/2} \\
&+ \frac{\Delta x^4}{384} T_{xxxx,i-1/2} + \frac{\Delta x^5}{3840} T_{xxxxx,i-1/2}
\end{aligned} \tag{26}$$

$$\begin{aligned}
T_{i-1} = T_{i-1/2} &- \frac{\Delta x}{2} T_{x,i-1/2} + \frac{\Delta x^2}{8} T_{xx,i-1/2} - \frac{\Delta x^3}{48} T_{xxx,i-1/2} \\
&+ \frac{\Delta x^4}{384} T_{xxxx,i-1/2} - \frac{\Delta x^5}{3840} T_{xxxxx,i-1/2}
\end{aligned} \tag{27}$$

Substituting these series expansions into Eqn. (18), again canceling the common terms with opposite signs, and making use of Eqn. (17), we obtain

$$\tau_i = \frac{\Delta x^2}{24} \frac{(D_{i+1/2} T_{xxx,i+1/2} - D_{i-1/2} T_{xxx,i-1/2})}{\Delta x} + O(\Delta x^4). \tag{28}$$

This is the truncation error for the arithmetic average. Notice that when $\Delta x \rightarrow 0$ this expression (Eqn. (28)) is equivalent to

$$\tau_i = \frac{\Delta x^2}{24} [(DT_{xxx})_{x,i}] + O(\Delta x^4), \tag{29}$$

or

$$\tau_i = \frac{\Delta x^2}{24} [D_{x,i} T_{xxx,i} + D_i T_{xxxx,i}] + O(\Delta x^4), \tag{30}$$

which is identical to the truncation error for the harmonic average.

Note: This analysis clearly shows that when the mesh resolution is fine enough, the two procedures are identical. This finding will be verified numerically in the following section.

5 Numerical results

5.1 Moving-front Single-material test

We solve Eqn. (1) in $[0, 1]$ with $T(0, t) = 2.0$, $T(1, t) = 0.1$, and $T(x, 0) = 0.1$. With these settings, the nonlinear conductivity term creates a moving

wave front. The front locations are shown in Figures 3,5, and 8 for different conductivity models and non-linearity.

Figures 3,5, and 8 show solutions at $time = 0.08$ with different mesh resolutions for $a = 3, 2$ and 1 respectively. As we can see from these figures, the harmonic average is very inaccurate for predicting the front location when a coarser mesh is used especially with larger a 's. Figures 4,6, and 9 show the errors committed by the two methods again for $a = 3, 2, 1$. The errors are calculated based on the comparison of the computed solution to a reference solution (i.e, a reference solution for $a = 3$ is generated with 3200 grid points). Figures 4,6, and 9 indicate second order convergence (in space) with the mesh refinements. Clearly, the harmonic average commits more error for coarser grids. On the other hand, for a very fine mesh the errors from the two methods are in the same order. This can be seen in Figure 7. This conclusion is also consistent with our truncation error analysis.

Another key observation from the error plots (Figures 4,6, and 9) is that the increase in nonlinearity(i.e, $a = 1, 2, 3$) means more error in both methods for the same amount of grid points. This behavior can also be verified by considering our truncation error analysis. For instance, we can see this by considering the truncation terms, i.e, for the harmonic average for $a = 1, 2, 3$;

$$\tau_i^{a=1} = \frac{\Delta x^2}{24} [T_{xxx,i} - TT_{xxx,i}] + O(\Delta x^4), \quad (31)$$

$$\tau_i^{a=2} = \frac{\Delta x^2}{24} [2TT_{xxx,i} - T^2T_{xxx,i}] + O(\Delta x^4), \quad (32)$$

and

$$\tau_i^{a=3} = \frac{\Delta x^2}{24} [3T^2T_{xxx,i} - T^3T_{xxx,i}] + O(\Delta x^4), \quad (33)$$

where $D = T^a$ and $D_x = aT^{a-1}$ with $a = 1, 2, 3$. Then we obtain $\tau^{a=2} = T\tau^{a=1} + O(\Delta x^2)$ and $\tau^{a=3} = T^2\tau^{a=1} + O(\Delta x^2)$.

We derive two conclusions from this test case. *One* is that the harmonic average is not better than the arithmetic average in contradiction to the common belief in literature. *Second*, both methods are convergent and comparable with finer grids.

We also make the following observation regarding validation and uncertainty quantification. Both harmonic and arithmetic averaging have been shown to

be second order accurate in space (Eqns. (23) and (28)). However, if the validation or uncertainty quantification are done at coarse grids, then the conclusions about uncertainty and accuracy would be very different. Therefore it is important to have a converged solution before the validation or uncertainty quantification is performed.

5.2 Stationary-interface Multi-material test

In this test, we solve the same PDE (e.g, Eqn. (1)), but we use constant in time (discontinuous in space, e.g, the discontinuity is located at the cell edge) heat conduction coefficient, i.e,

$$D(x, t) = \begin{cases} 1000 & \text{if } x \leq 0.5 \\ 1 & \text{if } x > 0.5 \end{cases} \quad (34)$$

We solve this problem in the same domain and with the same boundary conditions as in the single-material test case.

The discontinuity in the conductivity term represents a heat flow from a high-conductive material to a low-conductive material. We implemented both averaging techniques on this problem. We remark that a similar problem is studied by Patankar [7] based on which it was suggested that the harmonic average is more accurate. Our results also favor the harmonic average for this test when coarser grids are used. Nonetheless, with a fine-enough mesh, both methods are comparable.

Figure 10 shows the time history of the solution up to the steady state. The temperature builds up quickly in the high conductivity region (i.e, $x \leq 0.5$), then slowly diffuses to the low conductive material. Figure 10 is produced using 800 mesh points. We see that both methods give almost identical solutions. However the arithmetic average is slightly worse for coarser grids (i.e, Figure 11 with 20 points). This can be seen more clearly from Figure 12 which compares the errors committed by the two methods at different times. Notice that the error (especially for the arithmetic average) is higher at the front where the conductivity term changes dramatically. Also, Figure 12 shows that errors for both methods first grow in time during the transient, and then decrease as the solution approaches steady state. This is because

we have both temporal and spatial errors added during the transient, yet the temporal errors disappear at the steady state.

Figure 13 shows the log plots of the errors at different times. We observe from Figure 13 that during the transient the errors from both methods are within an order of magnitude of each other. However, when the steady state is reached and we have a diffusion coefficient that is constant from cell edge to cell edge, both assumptions of the harmonic average sub-grid model are met. In this case, the harmonic average is *many magnitudes* more accurate than the arithmetic average.

Figure 14 shows convergence analysis. Clearly both methods are second order with the mesh refinement. Finally, Figure 15 tells us that the harmonic average is better for coarser grids, yet both methods are good for a fine grid. We remark that we had the opposite conclusion in the first test (i.e, the arithmetic average was better for coarser grids, refer to Figure 7).

6 Conclusion

We investigated the effect of the choice between the harmonic and arithmetic averaging of the heat conduction coefficient on the heat transfer phenomena. We concluded that one should not favor one method over the other, because with a fine-enough mesh they are identical regardless of the model problem. However, we want to note that when using coarse grids one method can be better than the other depending on the model problem we are solving. For instance, in the single-material test, we found that the harmonic average is very inaccurate (refer to Figure 7). On the other hand, the harmonic average is more accurate in the multi-material test (refer to Figures 15 and 13). It is important to note that many validation and uncertainty runs are done on coarse grids. Thus, in this case, one has to be very careful when choosing the averaging technique.

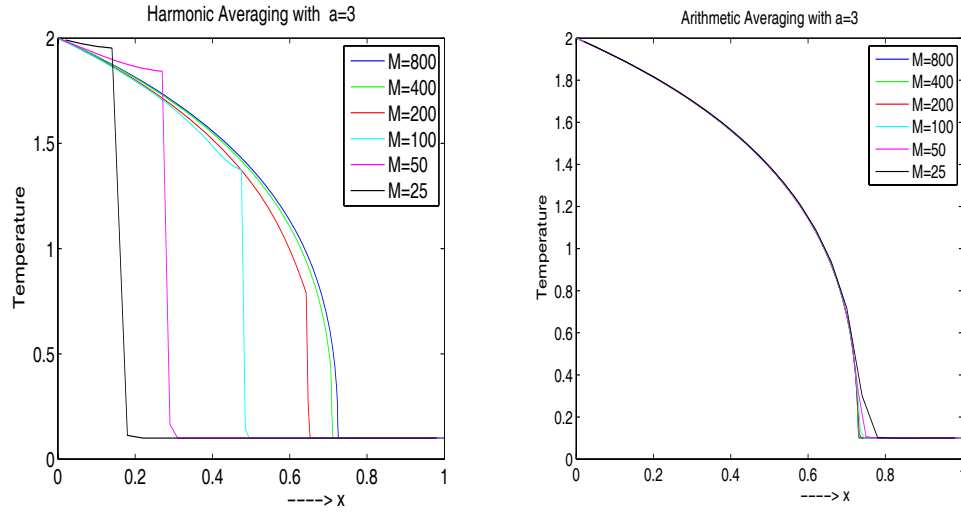


Figure 3: Comparison of the harmonic and arithmetic average for $a = 3$. Final run $time = 8 \times 10^{-2}$

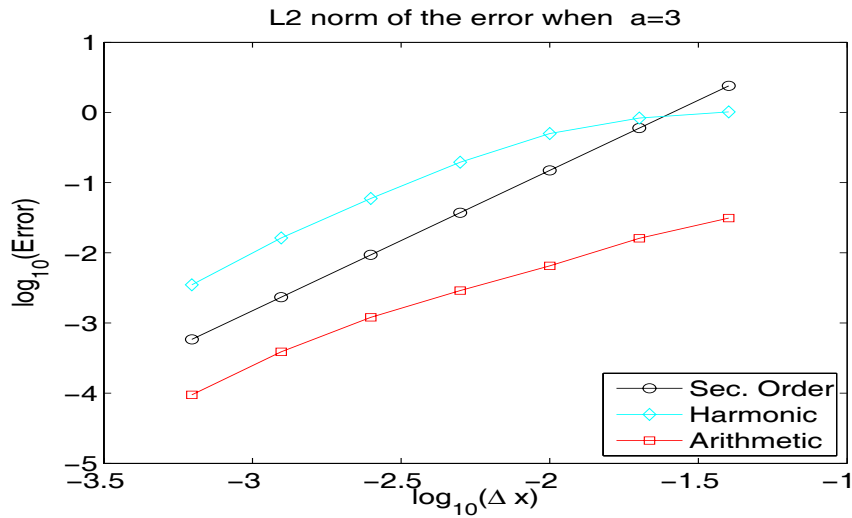


Figure 4: Comparing L2 norm of the errors committed by the two methods at $time = 8 \times 10^{-2}$.

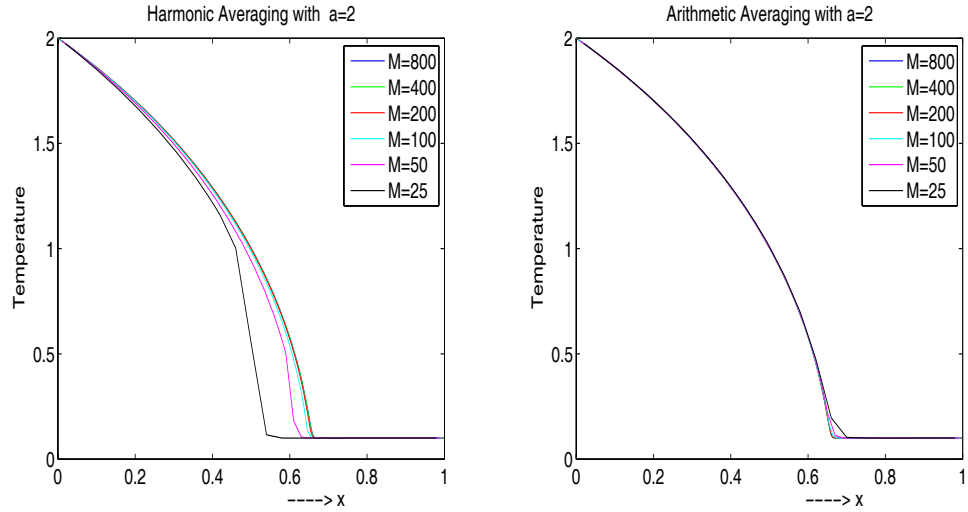


Figure 5: Comparison of the harmonic and arithmetic average for $a = 2$. Final run $time = 8 \times 10^{-2}$

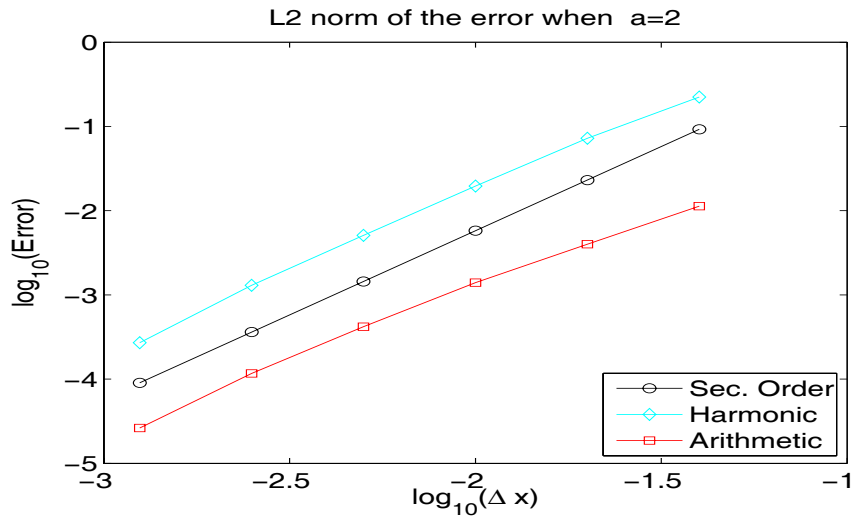


Figure 6: Comparing L2 norm of the errors committed by the two methods for $a = 2$ and $time = 8 \times 10^{-2}$.

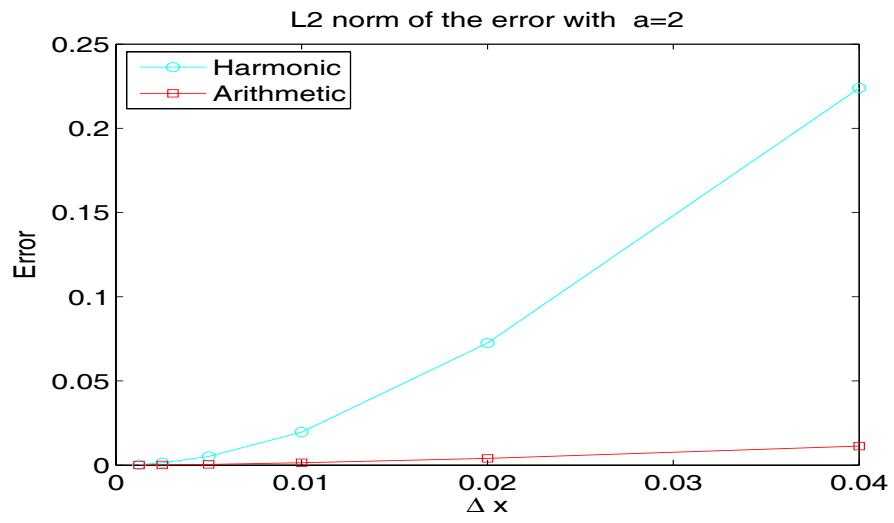


Figure 7: L2 norm of the errors committed by the two methods for $a = 2$ and $time = 8 \times 10^{-2}$. No log scale is used.

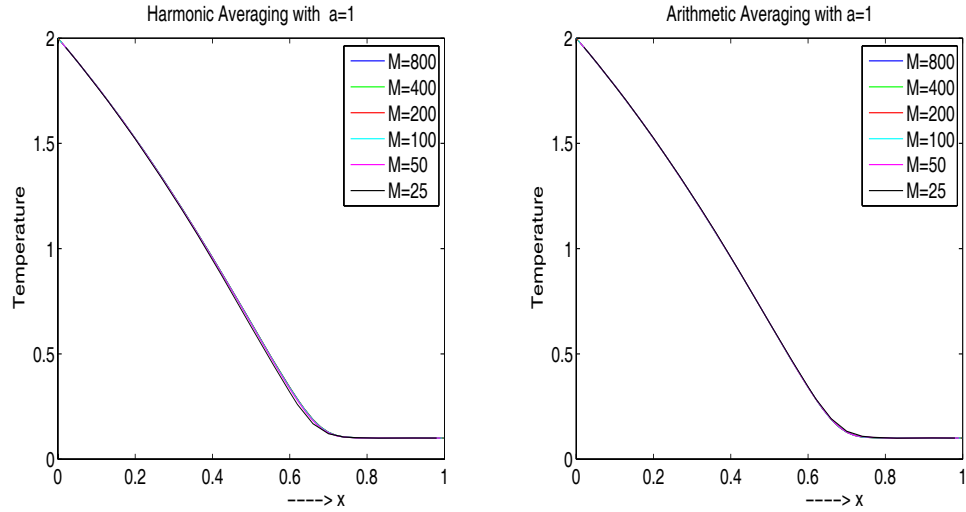


Figure 8: Comparison of the harmonic and arithmetic average for $a = 1$. Final run $time = 8 \times 10^{-2}$

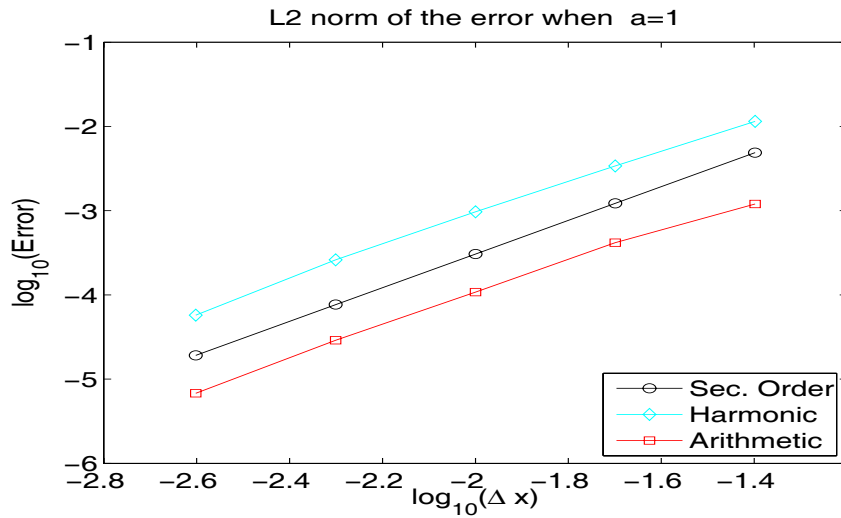


Figure 9: Comparing L2 norm of the errors committed by the two methods for $a = 1$ and $time = 8 \times 10^{-2}$.

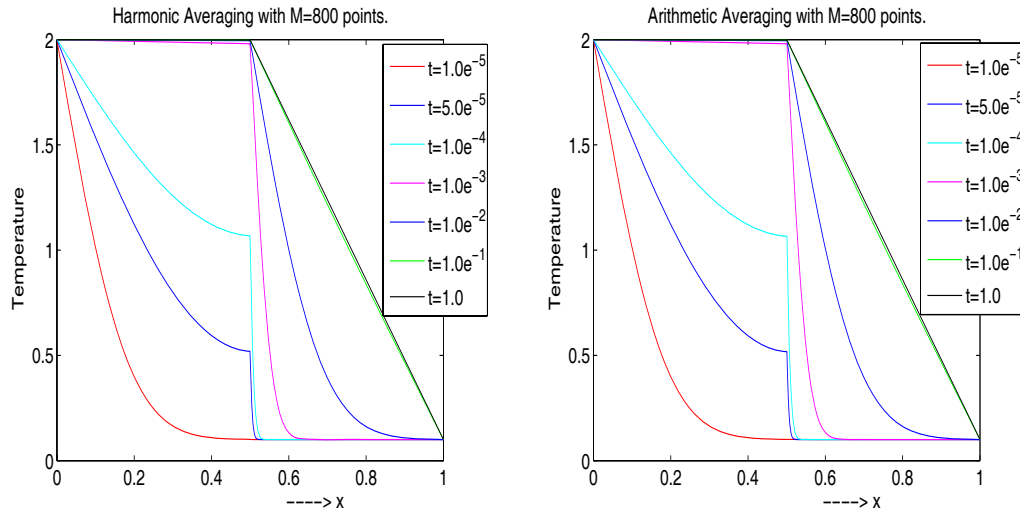


Figure 10: Time history of the solution by the two methods to the problem 5.2. The solution reaches the steady state at $time \approx 1.0$.

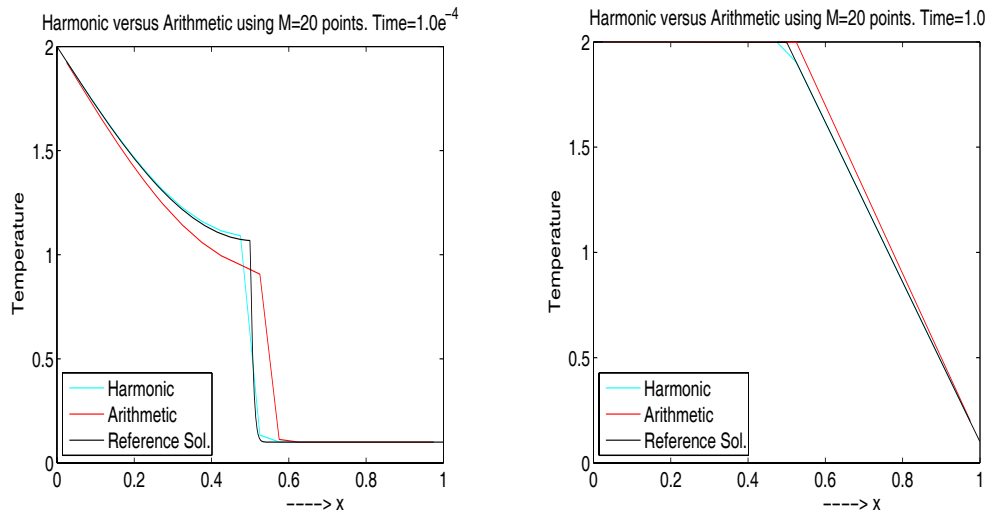


Figure 11: Comparing coarse runs from the two averaging against the reference solution. The left figure corresponds a transient solution, the right figure corresponds the steady state solution.

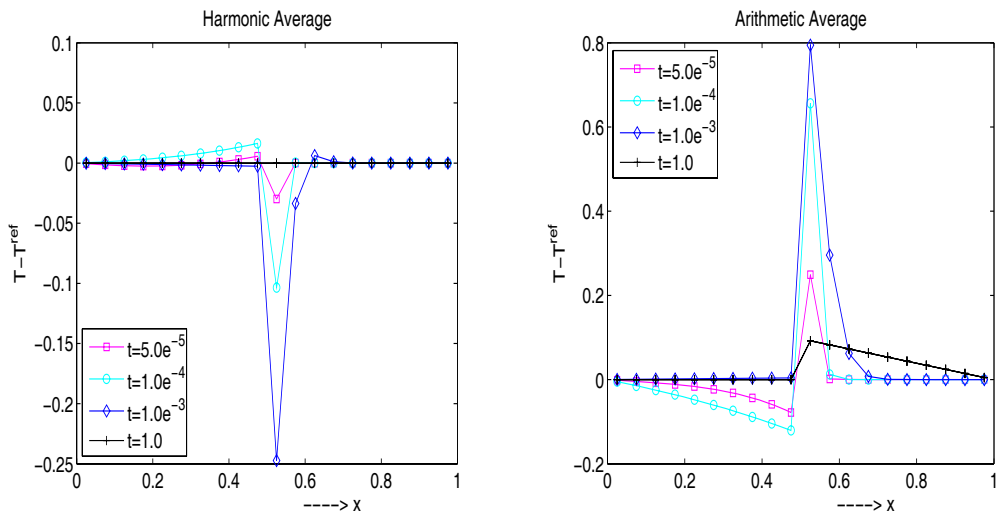


Figure 12: Errors at different times by the two methods when comparing the coarse ($M = 20$ grid points) solution to the fine ($M = 800$ grid points) solution.

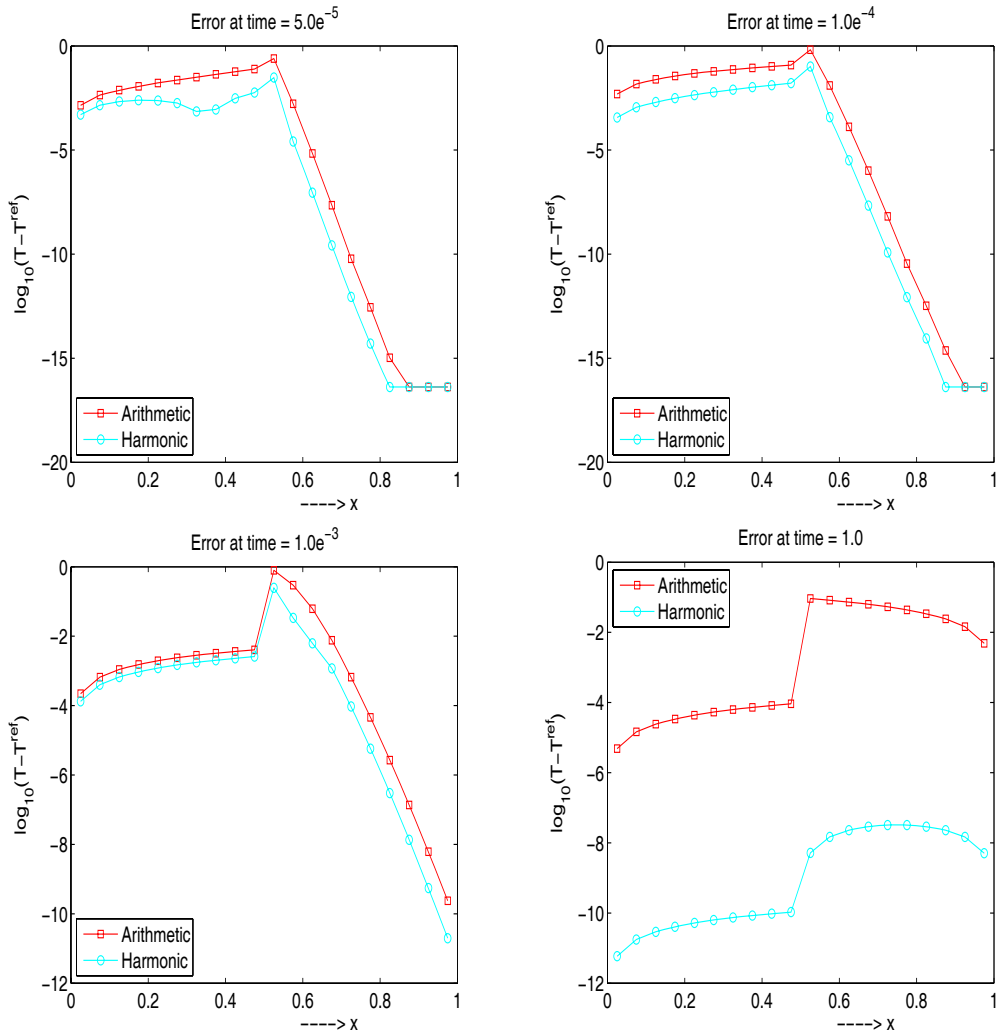


Figure 13: Errors by the two methods when comparing the coarse ($M = 20$ grid points) solution to the fine ($M = 800$ grid points) solution. Log scale is used in the y-coordinate direction.

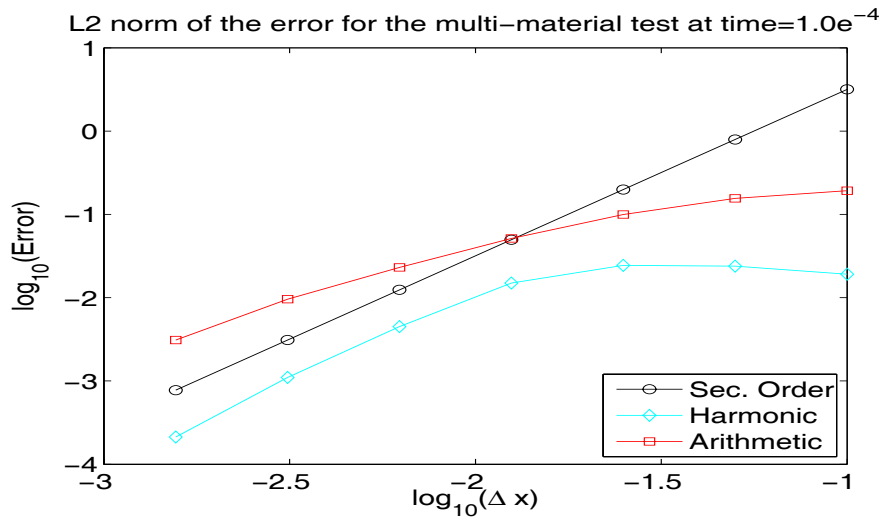


Figure 14: Convergence plots for the harmonic and arithmetic average when solving the multi-material test problem.

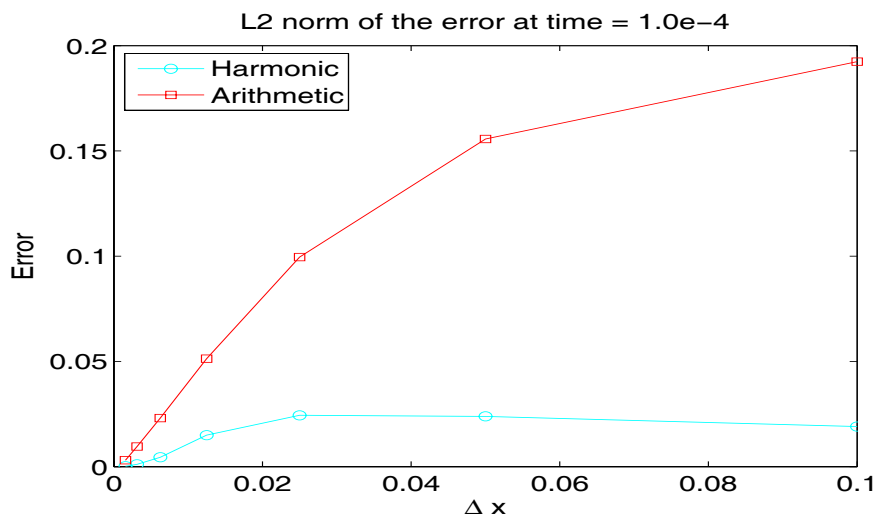


Figure 15: L2 norm of the errors when solving the multi-material test problem at $time = 1 \times 10^{-4}$. No log scale is used.

References

- [1] A. G. Hansen, M.P. Bendsoe, and O. Sigmund. Topology optimization of heat conduction problems using the finite volume method. *Struct. Multidisc. Optim.*, 31:251–259, 2006. [4.2](#)
- [2] D. A. Knoll and D. E. Keyes. Jacobien-free newton krylov methods: a survey of approaches and applications. *J. Comput. Phys.*, 193:357–397, 2004. [4](#)
- [3] E.W. Larsen and G. C. Pomraning. Asymptotic analysis of nonlinear marshak waves. *SIAM J. Appl. Math.*, 39:201–212, 1980. [3](#)
- [4] R. J. Leveque. *Finite Volume Methods for Hyperbolic Problems*. Cambridge University Press , Texts in Applied Mathematics, 1998. [4](#)
- [5] R.E. Marshak. Effect of radiation on shock wave behavior. *Phys. Fluids*, 1:24–29, 1958. [3](#)
- [6] G. L. Olson and J. E. Morel. Solution of the radiation diffusion equation on an AMR eulerian mesh with material interface. In *Technical Report LA-UR-99-2949*, 1999. Los Alamos National Laboratory (PDF available from author upon request). [4.2](#)
- [7] S.V. Patankar. *Numerical heat transfer and fluid flow*. Hemisphere, New York, 1980. [2](#), [5.2](#)
- [8] J. C. Strikwerda. *Finite Difference Schemes Partial Differential Equations*. Wadsworth & Brooks/Cole, Advance Books & Software, Pacific Grove, California, 1989. [4.3](#)
- [9] J.W. Thomas. *Numerical Partial Differential Equations I (Finite Difference Methods)*. Springer-Verlag New York, Texts in Applied Mathematics, 1998. [4](#), [4.3](#)
- [10] J.W. Thomas. *Numerical Partial Differential Equations II (Conservation Laws and Elliptic Equations)*. Springer-Verlag New York, Texts in Applied Mathematics, 1999. [4](#)